

MEASUREMENTS AND MODELLING ON A HIGH-POWER, LOW FREQUENCY PARAMETRIC ARRAY

C A Hamm (1), P Hines (2)

(1) Guigné International Ltd, Newfoundland, Canada

(2) Defence Research Establishment Atlantic, Nova Scotia, Canada

1. INTRODUCTION

Guigné International Limited (GIL) was commissioned by Defence Research Establishment Atlantic (DREA) to design and construct a high-power, low frequency parametric array. The parametric array, referred to as PATS (Parametric Array Transmit System), serves as the transmit head in an open-ocean research system developed at DREA [1]. The parametric sonar yields a wide bandwidth signal from a small aperture sonar, with virtually no sidelobes. The principle disadvantage of any parametric array is its inherent inefficiency, which is on the order of 1%. In any system design, this extreme inefficiency must be weighed against the merits of the parametric array approach. In the present case, operational requirements made the parametric array the preferred choice. Although the use of parametric arrays is fairly common, few have been constructed to operate at such high power levels and low frequencies as has PATS. The parametric array was designed to operate across a difference frequency band of 1 kHz to 10 kHz using a primary center frequency of 100 kHz. The maximum primary source level of the array is 243 dB re 1 μ Pa@1m. In this paper the PATS design is outlined, the calibration methods and calibration facility are described, and the results of the first set of tank measurements are presented.

2. THEORY

The fundamental principles of the parametric array were first presented in a paper by Westervelt [2], in which he described the non-linear interaction of sound in water and the subsequent generation of sound at frequencies other than those transmitted. Briefly, if two intense sound beams are coaxially transmitted into water, the non-linearity of the water medium generates secondary frequencies which are the sum and difference of the primary propagation frequencies. For example, a pulse of the form

$$S(t) = A \sin(f_0 \cdot t) \sin(f_m \cdot t) \quad (1)$$

consists of primary frequencies at $f_{p1}=f_0+f_m$ and $f_{p2}=f_0-f_m$. Transmitting a pulse defined by Equation (1) yields a sum and difference frequency at $f_s=f_{p1}+f_{p2}$ and $f_d=f_{p1}-f_{p2}$, respectively. In practical applications, absorption attenuates the sum frequency at small distances from the transmitter and it is the difference frequency which is of principle interest. In general, the sound pressure level and the beam pattern at the difference frequency is a complex function of transducer aperture and source level, the choice of primary and difference frequencies, and the properties of the medium. The literature contains a plethora of useful references for the interested reader (See for example, [3],[4],and [5] and the references therein.) Moffett and Mellen [5] state that the operating regime of a parametric array can approach one of four limits. These limits depend on whether the array length is terminated by small-signal absorption or non-linear absorption, and whether array termination occurs in the near-field or the far-field of the primary beam. For the present case, the array is near-field limited and approaches the limit of non-linear absorption, although small-signal absorption has a non-negligible effect. Mellen and Moffett [6] have modelled such an array. They write the difference frequency pressure $P(r, \theta, \phi)$ in spherical polar coordinates as:

HIGH POWER, LOW FREQUENCY PARAMETRIC ARRAY

$$P(r, \theta, \phi) = \beta \frac{(P_o R_o k)^2 \pi}{4 \pi \rho c^2} \int_0^\pi d\theta' \sin \theta' \times \int_0^{2\pi} d\phi' D_o^2(\theta', \phi') I(\cos v) \quad (2)$$

where β is the non-linearity parameter (3.5 for water), k is the difference frequency wavenumber, ρ is the ambient fluid density, c the sound speed, and v is the angle between source point and observer. The function $I(\cos v)$ represents the range integration and is given by,

$$I(\cos v) = \int_0^\infty dr' U(r') \zeta^{-1} \exp[-2\alpha r' - jk(r' + \zeta)] \quad (3)$$

where the function $U(r')$ accounts for the non-linear absorption of the primary signal, the term $\exp(-2\alpha r')$ accounts for the small-signal absorption at the primary frequency, r' is the distance from the transducer to the source point, and ζ is the range from the source point to the observation point. The model results presented throughout this paper were obtained by solving Equation (2) using the method outlined in [6].

3. DESCRIPTION OF SONAR

In this section we present an overview of the mechanical, electrical and acoustic design of the PATS sonar.

The transmit array consists of nine square piston transducers made of PZT-4 ceramics arranged in a 3-by-3 grid. The design specification and performance requirements were provided by GIL, and were designed, manufactured, and tested by International Transducer Corp. (ITC), Santa Barbara, USA. Each transducer has a 30 kHz bandwidth centred on 100 kHz. Individual transducers are 13.5 cm per side, but have an active area of 11 cm per side. This gives an active area of 1089 cm² for the nine transducer array. The full array has a directivity index at 100 kHz of approximately 38 dB. The transducer design allows for up to 2 W/cm² radiated intensity when operated at duty cycles less than 3%. A primary source level of 242 dB re 1 μ Pa@1m was predicted with a radiated intensity of 2 W/cm² over the active area.

The PATS system contains four power amplifiers designed to operate at 100 kHz having a bandwidth from 60-300 kHz. Each amplifier is capable of creating a 2000 W RMS pulse, into a 50 ohm load, with a maximum pulse duration of 300 ms. The amplifiers connect to the projectors through a transformer-based power combiner unit. In this arrangement up to 8 kW is available to the transducers. The output of the power combiner goes to all nine projectors wired in parallel. For the calibration measurements a cylindrical pressure housing contained five 55 Ah gel cell 12 V batteries. Waveforms are passed to the head via an underwater coaxial cable from a bench mounted arbitrary waveform generator. The signal input range is 2 V peak-to-peak for full output power. The electronics is housed in an anodized cast aluminum body with a maximum operational depth of 300 m. Internal mechanisms permit the amplifier heat sinks to couple directly to the housing wall. The approximate weight of the main housing is 200 kg.

Figure 1 shows the measured impulse frequency response for the integrated sonar assembly. This was obtained using a 5 μ s pulse (200 kHz bandwidth). The results in Figure 1 show a centre frequency of 100 kHz with a -3 dB bandwidth of 30 kHz. Since the highest difference frequency is approximately equal to the primary bandwidth this allows a useable difference frequency bandwidth of 30 kHz. For these

HIGH POWER, LOW FREQUENCY PARAMETRIC ARRAY

experiments difference frequency measurements were limited to a maximum of 15 kHz.

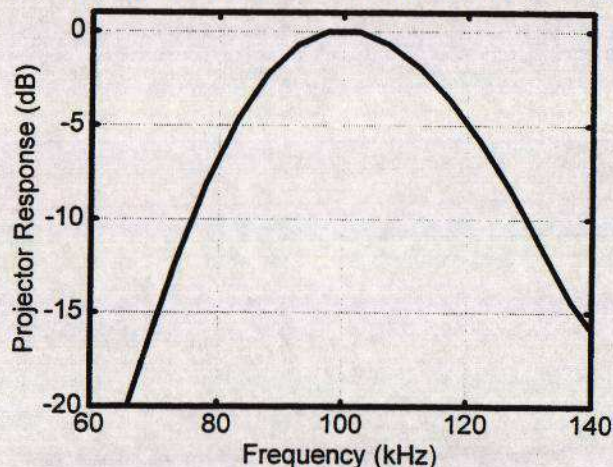


Figure 1: System impulse response.

4. TEST FACILITY AND EXPERIMENTAL SETUP

4.1 Test Facility

To calibrate the array, a facility was required that was long enough to allow measurements in the far-field of the array at the primary frequencies and the difference frequencies. It also had to be deep and wide enough to prevent multipath reflections from interfering with direct arrivals. Furthermore, due to the narrow beam pattern of the array, the mounting platform had to be stable and its positioning had to be accurately controlled. Collectively, these requirements were satisfied using the Institute for Marine Dynamics (IMD) tow-tank [7], St. John's, Newfoundland, Canada.

The IMD tow-tank is a freshwater facility measuring 200m×12m×7m (L×W×D). However, for the present experimental configuration the maximum range between source and receiver was 100 m. This limit resulted from interference of multipath arrivals with the direct arrival. At the time of calibration the water temperature was 5° C.

4.2 Experimental Setup

The calibration setup is shown in Figure 2. The sonar assembly was positioned at mid-depth on a tower, purpose-built for the calibration. The acoustic axis was aligned with the tank centre line. Hydraulic jacks were fitted to the frame to allow fine angle adjustments. A Bruel and Kjaer model 8105 hydrophone was suspended from a stable, rolling gantry which spanned the tank width. The hydrophone sensitivity variation is less than 4.5 dB across the frequency band 0.1 Hz to 100 kHz. A 1 kg weight suspended 2 m below the hydrophone was used to reduce motion.

4.3 Data Acquisition

The transmit control and receive data acquisition systems were located at one end of the tank and synchronised by a trigger pulse. This enabled positive identification of direct and multipath arrivals through known propagation delays. Hydrophone signals were passed into a Bruel and Kjaer model 2635 charge amplifier. These signals were acquired using a Hewlett-Packard type 54600 digital oscilloscope. Data analysis was performed on a PC using MATLAB® software.

HIGH POWER, LOW FREQUENCY PARAMETRIC ARRAY

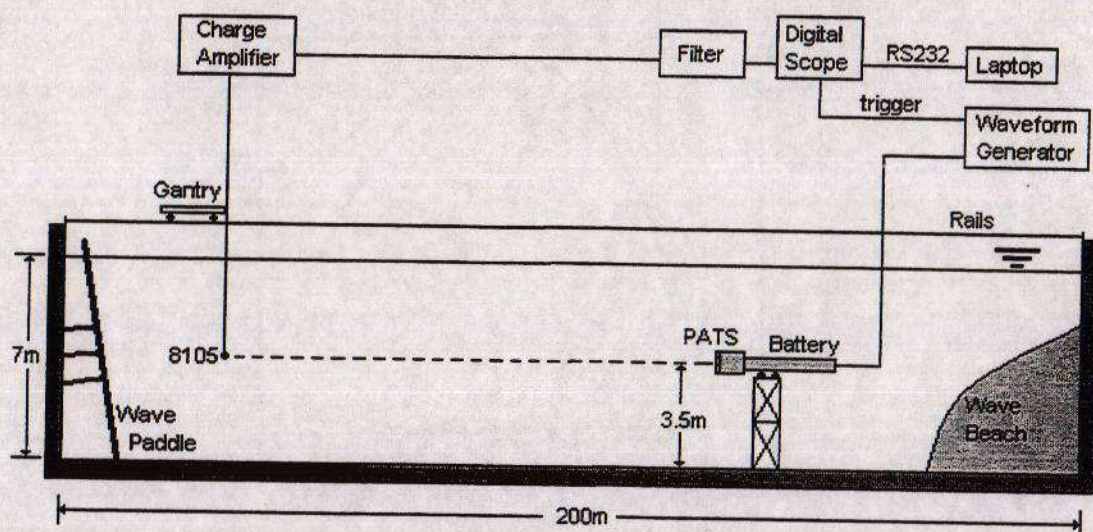


Figure 2: Institute for Marine Dynamics tank setup. Shown are the relative positions of sonar head and hydrophone, with block diagram of signal generation and data acquisition system.

5. RESULTS AND DISCUSSION

In this section we present the experimental results. Characterising the parametric array requires measurements at the primary frequencies as well as at the difference frequencies. We shall begin by examining the primary frequency measurements.

5.1 Primary Frequency Measurements

Figure 3 shows the primary source level SL_p measured at 100 kHz, plotted as a function of input power. The source level was calculated from the sound pressure level (SPL) measured at range R using the equation,

$$SL = SPL + 20 \log_{10} R + \alpha R \quad (4)$$

where α is the absorption coefficient at the primary frequency in dB m^{-1} . Equation (4) is only valid only for measurements made in the limit of spherical spreading. This region is defined as $R \gg 2R_0$, where R_0 is the Rayleigh Distance, defined as the ratio of transducer area to primary wavelength [8]. For the present experiment, measurements were made at ranges of R from 50 m to 80 m and SL_p estimates were consistent to within 0.5 dB.

Referring to Figure 3 we see that for power input less than 2 kW, SL_p increases 3 dB for a doubling of input power indicating that the acoustic output is increasing linearly with input power. At 2 kW input power the onset of saturation is visible as the acoustic output no longer increases linearly with input power. Finally, above 5 kW the array is fully saturated and increasing the input power yields no additional acoustic output. From [9] a parametric array is said to be saturated when the scaled source level, $SL_0^* = 281 \text{ dB re } 1\mu\text{Pa}\cdot\text{m}\cdot\text{kHz}$, where

HIGH POWER, LOW FREQUENCY PARAMETRIC ARRAY

$$SL_o^* = SL_p + 20 \log_{10} f_o(\text{kHz}) \quad (5)$$

which for the current experiment equates to $SL_p = 241 \text{ dB re } 1\mu\text{Pa}@1\text{m}$. This is consistent with the data of Figure 3.

Figure 4 shows the horizontal and vertical cross sections of the primary beam pattern. Measurements were made at 50 m range using a source level of $241 \text{ dB re } 1\mu\text{Pa}@1\text{m}$. Rectangular pulses of 0.2 ms duration were used to eliminate multipath interference from tank boundaries. Beam pattern measurements were made along a line perpendicular to the acoustic axis. For displacements up to 2 m from the acoustic axis the measurements were taken at 20 cm intervals; For displacements of 2 m to 5 m, from the acoustic axis, measurements were taken at 50 cm intervals. These displacements correspond to angular separations of approximately 0.23 and 0.57 degrees, respectively. The horizontal and vertical beam patterns were virtually identical on the main lobe, and within 1 dB of one another on the first sidelobe. The beamwidth at the -3 dB points is approximately 2 degrees. Measurements beyond the first sidelobe were not possible due to interference from boundary reflections.

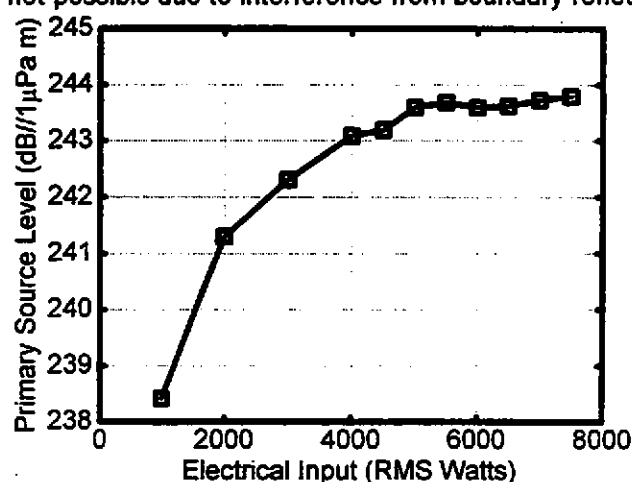


Figure 3: Primary source level, SL_p , versus input electrical power.

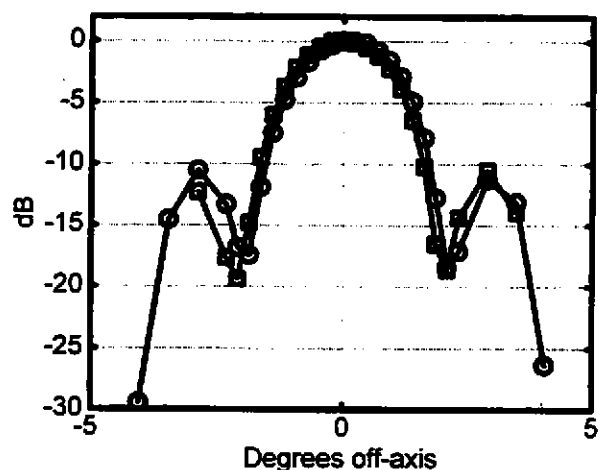


Figure 4: Primary beam pattern in horizontal (o) and vertical (□) cross section. Data taken at 50 metres range, $SL_p = 241 \text{ dB re } 1\mu\text{Pa}@1\text{m}$.

5.2 Difference Frequency Measurements

Figure 5 shows the difference frequency horizontal beam patterns for 6 kHz and 10 kHz at 50 m range. The absence of sidelobes and the decrease in beamwidth with increasing frequency are both characteristic of parametric arrays.

Figure 6 shows a comparison between beam pattern measurements at $f_d = 10 \text{ kHz}$ and the prediction based on Equation (2). The agreement between theory and data is within 2 dB for angles less than 2.5 degrees measured from the acoustic axis. However, for angles greater than about 2 degrees the slope of the modelled beam pattern is less than the measured values such that at 5 degrees off-axis the model results are 5 dB greater than the data. The half-power full-beamwidths for both model and data are 2.1 ± 0.1 degrees.

HIGH POWER, LOW FREQUENCY PARAMETRIC ARRAY

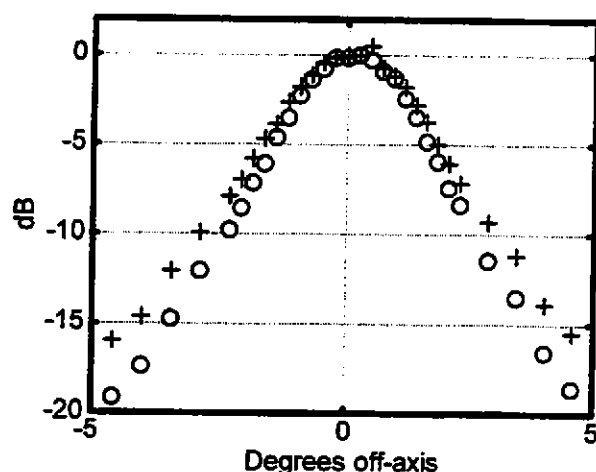


Figure 5: Difference frequency beam patterns. Shown are data at 50m for difference frequencies of 6 kHz (+) and 10 kHz (o).

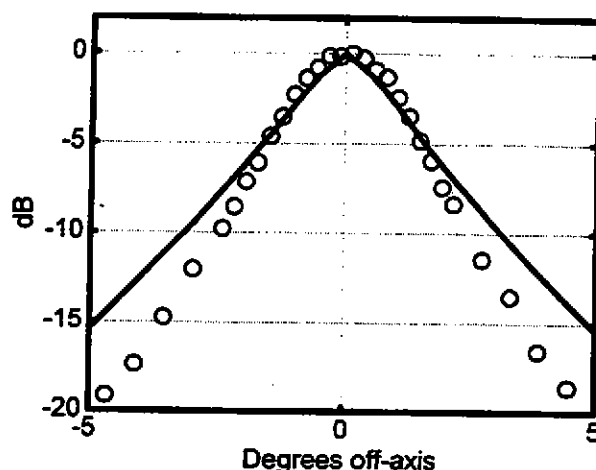


Figure 6: Comparison of 10kHz difference frequency beam pattern at 50 m range (o) with theoretical prediction (solid line).

Measurements of sound pressure level taken along the acoustic axis at frequencies of 6 kHz, 10 kHz and 15 kHz are presented in Figure 7. These measurements were taken using a SL_p of 242 ± 1 dB re $1 \mu\text{Pa}@1\text{m}$. Axial measurements at 10 kHz were repeated and differences between data sets were confined to 0.5 dB. The 15 kHz data indicate the peak sound pressure level at the difference frequency, SPL_d , occurs at approximately 10 m suggesting that the array is terminated in the near-field. (The Rayleigh distance for this array equals 8.7 m). Furthermore, recalling from Equation (5) the parametric array is saturation limited for these primary source levels. This suggests the model of [6] is appropriate.

Figure 8 shows the model results calculated as a function of axial range, for a source level of 242 dB re $1 \mu\text{Pa}@1\text{m}$ at a difference frequency of 15 kHz. The 15 kHz data from Figure 7 is also replotted in the figure. Although the slope is consistent for both model and data, the model over-estimates the measured levels by approximately 14 dB. Measurements were repeated several times, the integrity of the data acquisition system was verified, and computer coding was validated by comparing model outputs to benchmark cases contained in the literature. The authors can offer no explanation for the discrepancy between the model and data at this time.

HIGH POWER, LOW FREQUENCY PARAMETRIC ARRAY

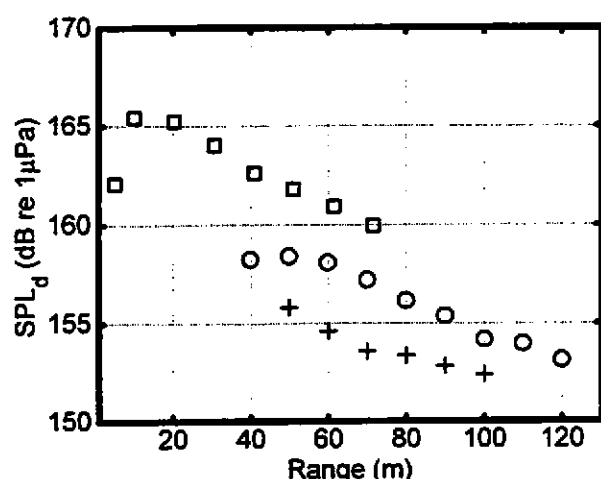


Figure 7: Axial SPL_d vs. range for difference frequencies 6 kHz (+), 10 kHz (o), and 15 kHz (□).

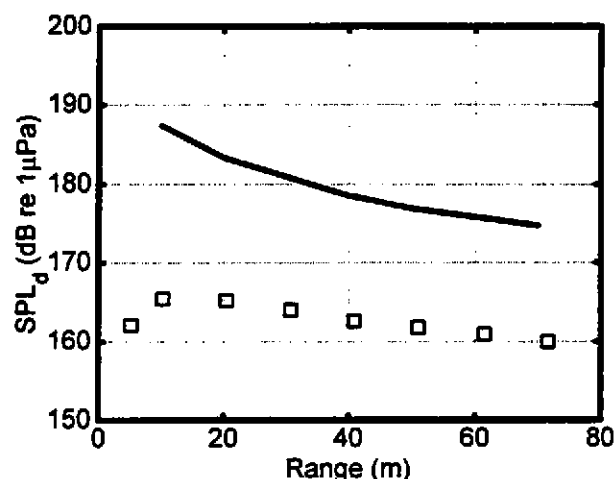


Figure 8: The 15 kHz prediction for axial sound pressure levels based on Equation 2 (solid line) and 15 kHz data (□).

6. FUTURE WORK

Future work will include testing PATS operated at lower primary source levels such that the absorption limited regime can be studied. These tests are planned to take place in DREA's Barge Facility [10] which provides a fully free-field, saltwater environment. Measurements will be taken over a wider range of frequencies — 1 kHz to 30 kHz. Further examination of the literature will take place to ensure the most appropriate model is being used.

7. CONCLUSIONS

In this paper the results of an acoustic calibration of a high power, low frequency, parametric array were presented. The calibration data were compared to a parametric array model contained in the literature [6]. Critical to the calibration was the use of a large indoor tank facility (200m×12m×7m) in which the measurements were performed. The sound pressure level was measured at the primary frequency (100 kHz) as well as at difference frequencies of 6, 10, and 15 kHz. The beam pattern was also measured at the primary frequency and at difference frequencies of 6 and 10 kHz.

The onset of acoustic saturation occurred at a primary frequency source level of 241 dB re 1 μ Pa@1m. This is consistent with theoretical estimates.

The measured beam pattern for a 10 kHz difference frequency agreed with the model to within 2 dB out to angles of 2.5 degrees from the acoustic axis. For angles greater than approximately 2.5 degrees off-axis the modelled beam pattern overestimates the measured results. At 5 degrees the theoretical prediction is approximately 5 dB greater than the data. The half-power full-beamwidths for both model and data are approximately 2 degrees.

The relative range dependence of the modelled and measured sound pressure level at 15 kHz is in good

HIGH POWER, LOW FREQUENCY PARAMETRIC ARRAY

agreement for ranges from 20 to 70 m. At shorter ranges the model is no longer valid. The absolute level of the model is approximately 14 dB higher than the data. At this time, the authors can offer no explanation for this discrepancy.

8. REFERENCES

- [1] P C Hines, W Cary Risley, and Martin P O'Connor, A wideband sonar for underwater acoustics measurements in shallow water, *Oceans 98*, Sept. 1998, Nice, France (accepted paper).
- [2] P J Westervelt, Parametric acoustic array, *J. Acoust. Soc. Am.*, **35**, 1963, 535-537.
- [3] B V Smith, Introduction to non-linear acoustics and the parametric array, *Proc. I.O.A.* Vol 14 Part 3, 1992, 1-26.
- [4] M B Moffett, and R H Mellen, W. Konrad, Parametric sources of rectangular aperture, *J. Acoust. Soc. Am.* **63** (5), 1978, 1326-1331.
- [5] M B Moffett, and R H Mellen, Model for parametric acoustic sources, *J. Acoust. Soc. Am.* **61** (2), 1977, 325-337.
- [6] R H Mellen, and M B Moffett, A numerical method for calculating the nearfield of a parametric acoustic source, *J. Acoust. Soc. Am.* **63** (5), 1978, 1622-1624.
- [7] N E Jeffrey, and D C Murdey, The NRC Institute for Marine Dynamics: your new national facility 1986, Presented at the Canadian Shipbuilding and Ship Repair Conference, Montreal, 1986 (see also <http://www.nrc.ca/imd/>).
- [8] L E Kinsler, A R Frey, A B Coppens and J V Sanders, Fundamentals of Acoustics, 3rd ed., John Wiley and Sons, 1980, page 177
- [9] M B Moffett, and R H Mellen, Nearfield characteristics of parametric acoustic sources, *J. Acoust. Soc. Am.* **69** (2), 1981, 404-409.
- [10] G W McMahon, and C V Sheffer, Microcomputer-controlled transducer calibration facilities at the Defence Research Establishment Atlantic, *Proc. I.O.A.* Vol 6 Part 5, 1984, 96-105.

ACKNOWLEDGMENTS

The authors express their sincere thanks to GIL staff Dave Hicks and Melvin Hicks, and Dan King, for technical support and advice during the calibration exercise. M H and D K were also members of the PATS sonar design team. We are deeply indebted to Mr. Spence Butt who performed many dives to install and align the sonar. We also express our gratitude to Mr. Noel Murphy, the IMD Industrial Liaison Officer at IMD, for allowing us the use of the IMD facility and accommodating our difficult schedule.